Revista Mexicana de Física
ISSN: 0035-001X
rmf@ciencias.unam.mx
Sociedad Mexicana de Física A.C.
México

Cadena-Nava, R.D.; Martin-Mirones, J.M.; Vázquez-Martínez, E.A.; Roca, J.A.; Ruiz-García, J.
Direct observations of phase changes in Langmuir films of Cholesterol
Revista Mexicana de Física, vol. 52, núm. 5, noviembre, 2006, pp. 32-40
Sociedad Mexicana de Física A.C.
Distrito Federal, México

# Direct observations of phase changes in Langmuir films of Cholesterol

R.D. Cadena-Nava[a], J.M. Martin-Mirones[a], E.A. Vázquez-Martínez[a], J.A. Roca[b], and J. Ruiz-García[a,*]
[a] *Instituto de Física, Universidad Autónoma de San Luis Potosí, 78000 San Luis Potosí, S.L.P., México.*
[b] *Centre de Desenvolupament de Sensors, Instrumentació i Sistemes, Universitat Politecnica de Catalunya, Rambla de Sant Nebridi 10, E-0822, Terrasa, España.*

Recibido el 10 de febrero de 2006; aceptado el 6 de mayo de 2006

We report isotherm, Brewster angle (BAM), ellipsometry and atomic force microscopy (AFM) studies of Langmuir films of cholesterol. At low surface pressures the Langmuir monolayers of cholesterol show a gas(G)-liquid condensed (LC) coexistence region in the range of 10 to 40°C. On further compression, the pure untilted LC phase region is entered, denoted by a rapid increase in surface pressure. Then, the monolayer is over compressed up to the collapse pressure, which is denoted by a long constant-pressure plateau. BAM observations show that the long plateau resembles a coexistence region between a 2D monolayer and 3D crystallites. The thickness of the crystallites measured *in situ* by ellipsometry are in good agreement with AFM measurements on transferred films on mica, which also reveal details of the large-size crystallites formed during collapse. The shape of the crystallites resembled those of the cholesterol monohydrate, but we found that they break over time into long, thinner crystal bars of anhydrous cholesterol. This phenomenon takes place at all temperatures, although at 10 and 20°C, the initial monohydrate crystals are shallow and small enough to allow a ready formation of the anhydrous crystal bars. At the two higher temperatures the monohydrate crystals are quite large, avoiding their total fragmentation into anhydrous crystal bars. Our results show for the first time a direct evidence that the initial monohydrate crystals formed during monolayer collapse are metastable against the anhydrous-type crystal bars, but the former crystals seem to increase their stability with the higher temperature.

*Keywords:* Langmuir monolayers; Langmuir-Blodgett films; cholesterol; phase transitions.

Reportamos estudios por isotermas, microscopia de Angulo de Brewster (BAM), elipsometria y microscopia de fuerza atómica (AFM) de películas de Langmuir de colesterol. A presiones superficiales bajas las monocapas de Langmuir de colesterol muestran una región de coexistencia gas (G)-liquido condensado (LC) en el rango de 10 a 40°C. A mayor compresión, se entra a la región de la fase pura sin inclinación LC, denotado por un rápido incremento en la presión superficial. Después, la monocapa es sobre comprimida hasta la presión de colapso, la cual es denotada por un plato largo a presión constante. Las observaciones de BAM muestran que este plato parece una región de coexistencia entre la monocapa 2D y cristalitos 3D. El espesor de los cristalitos medidos in situ por medio de elipsometría está en buen acuerdo con las medidas de AFM de las películas transferidas a mica, las cuales también revelan detalles de los cristalitos de gran tamaño formados durante el colapso. La forma de los cristalitos corresponde a los de colesterol monohidratado, pero encontramos que ellos se rompen con el tiempo en largas y delgadas barras de colesterol anhídrido. Este fenómeno ocurre a todas las temperaturas, aunque a 10 y 20°C, los cristales monohidratados iniciales son achaparrados y suficientemente pequeños para permitir una fácil formación de las barras cristalinas anhídridas. A las dos temperaturas mas altas los cristales monohidratados son bastante grandes, evitando su fragmentación total a las barras cristalinas anhídridas. Nuestros resultados muestran por primera vez evidencia directa que los cristales iniciales monohidratados formados durante el colapso de la monocapa son metaestables frente a las barras cristalinas del tipo anhídrido, pero los primeros cristales parecen incrementar su estabilidad a temperaturas más altas.

*Descriptores:* Monocapas de Langmuir; películas Langmuir-Blodgett; colesterol; transiciones de fase.

PACS: 68.03.-g, 68.18.-g; 68.18.Jk; 68.37.Nq; 68.47.Pe

## 1. Introduction

Langmuir films, formed when a solution made of non-soluble amphiphilic molecules is spread by means of a solvent on the water surface, are of great interest in biology as model membranes [1], in molecular electronics [2] and in the fabrication of special electrodes [3] or biosensors [4]. As a consequence, Langmuir films and their air/solid derived Langmuir-Blodgett (LB) films have been the subject of intense research in the last decades. New techniques for their study have been introduced, for example, epifluorescence [5, 6], polarized, [7, 8] Brewster angle (BAM) [9, 10] and atomic force (AFM) microscopies [11], and X-ray diffraction at grazing angles (GIXD) [12, 13]. Using these techniques, it has been rediscovered [14-16] that Langmuir films show a rich polymorphism, where various phases (mesophases) have been shown to be two-dimensional analogs of smectic liquid crystalline phases. It has also been possible to resolve from mesoscopic structures down to the molecular order [16].

Up to now, most of the work on Langmuir films has focused on the isotherm part where there is only a monomolecular film, from low to moderate surface pressures, c.a. $\sim$35 mN/m. Only scattered efforts have been made the last three decades on monolayer collapse. The monolayer collapse, presumably the onset of multilayer formation, is often identified in isotherm measurements as the point where the surface pressure reaches a maximum, and either a spike (a sharp pressure drop) or a plateau is observed [16]. This point is normally called the "collapse pressure".

Collapse has also been reported to occur at lower surface pressures, when the system is compressed above the so-

called "equilibrium spreading pressure" (ESP) [15]. This is the pressure where the two-dimensional monolayer coexists with the bulk phase; therefore, above the ESP all monolayers are metastable and collapse should occur as the film relaxes toward the ESP. Lundquist reported a precollapse line in acetates and esters in the middle of the so-called superliquid (LS) phase region [17]. Smith and Berg [18] studied the collapse of nine different amphiphiles by measuring the change in surface pressure vs. time; they basically found that collapse of the films was consistent with a model of homogeneous nucleation and a subsequent growth of bulk surfactant fragments. Vollhardt et al. [19], in a series of papers, have studied the kinetics of "slow collapse" above the ESP following the decrease in area while maintaining a constant pressure. They suggested that the collapse mechanism is in agreement with a nucleation, growth and overlap of the nucleation centers.

Not only the collapse of small amphiphile molecules has been studied but also the collapse of large macromolecules. An interesting case is the collapse of polysiloxane films at the air/water interface. It has been found that isotherms show the formation of up to seven different plateaus. Godovski *et al.* [20] have shown that these plateaus correspond to a smooth collapse where a new layer is formed at each plateau. The initial growth of the second layer begins with the nucleation of three-dimensional islands, which spread in the form of ribbons, and so on.

From the theoretical standpoint, models for monolayer collapse by nucleation and growth [18, 19], and nucleation-growth-collision have been proposed [19], these theories consider the nucleation and growth and further overlapping of growing centers as the monolayer relaxes towards the equilibrium spreading pressure. From the microscopic understanding of collapse, it has been proposed that bulk nucleation proceeds only if defects are present [21, 22] and the growth of a solid phase is associated with a plastic deformation.

The study of the onset of multilayer formation at the collapse pressure can be important because it can give us clues to the mechanism of the formation of model flat multilayer membranes from Langmuir films and on its stability both at air/water and air/solid interfaces. In general, we can say that at collapse pressure there is a direct and strong formation of multilayers, while collapse just above the ESP could be thought of as a progressive and slower process for multilayer formation. However, a detailed study of the three-dimensional crystallite shape and microstructures formed during collapse is still missing.

On the other hand, cholesterol crystallization is of great importance in health issues. Cholesterol is the most abundant sterol in animal and human membranes and plasma lipoproteins. It is a precursor in the biosynthesis of bile salts and hormones. Recently, it has been shown that cholesterol together with sphingolipids form organized domains, lipid rafts [23, 24] that participate in distributing proteins to the cell surface, and is active in cell signal transduction and the activation of immune responses. However, abnormally high physiological levels of cholesterol may develop into detrimental precipitants containing cholesterol crystallites that are associated with atherosclerotic plaques [25-27], with rheumatoid arthritis, and with gallstones in the biliary system [28].

In atherosclerotic plaques, the cholesterol has the morphological form of crystal bars, which are apparently needle-shaped, but at higher magnification, they actually have a rectangular cross-section [29]. Normally, the tissue surrounding those bars is all necrotic (dead) debris. Cholesterol crystals are commonly found in association with inflammation when there is necrosis involved. Cholesterol crystals are also present in rheumatoid arthritis, but these crystals have a different shape from those found in atherosclerotic plaques; they are characterized by broad square or rectangular plate-like crystals with a notched corner, created by their propensity to adhere to one another's surfaces.

The nucleation of cholesterol crystals is also necessary in the formation of gallstones (lithiasis). Light and electron microscopy and synchrotron X-ray diffraction show that a high cholesterol-to-phospholipid ratio favors cholesterol crystallization [30-37]. Furthermore, an X-ray powder diffraction pattern obtained from early-formed filamentous crystallites of cholesterol in bile solution has been interpreted as possibly depicting an unknown crystalline polymorph of cholesterol [38].

In general, cholesterol shows two types of polymorphic crystals in bulk: monohydrate and anhydrous [39]. In water or at high humidity values, the stable form is the monohydrate form, which transforms into the high-temperature anhydrous form at 86°C. At low humidity values, the stable form is the anhydrous form, which shows a phase transition between two anhydrous forms at 39°C. GIXD experiments have shown that cholesterol self-assembles as a monolayer at the air/water interface and, upon compression, into an ordered monolayer film of trigonal symmetry *P3* but with low lateral order [40]. It has been reported recently that, upon further compression, cholesterol collapses to a trilayer composed of a highly crystalline bilayer in a rectangular lattice and a disordered top cholesterol layer [41], where there is a layer of ordered water between the top and middle sterol moieties, forming a crystalline hydrate.

In this work, we present isotherm, ellipsometry, BAM and AFM studies of Langmuir monolayers of cholesterol along their isotherms in the range of 10 to 40°C. We study its phase behavior, the collapse process and its bearing on cholesterol crystallization in health issues.

## 2. Experimental

Cholesterol (5-cholesteren-3$\beta$-ol ($C_{27}H_{46}O$), > 99% of purity) was purchased from Sigma-Aldrich (Sigma-Aldrich, St. Louis, MO, USA), and it was used without further purification. Chloroform (HPLC grade, 99.9%, Sigma-Aldrich, St. Louis, MO, USA) was used as a spreading and cleaning solvent. We also used ethyl alcohol (J.T. Baker, 99.9%,

Xalostoc, Mexico) absolute anhydrous as cleaning solvent. The subphase was deionized water (bioresearch grade water, 18.3 MΩ-cm of resistivity, NANOpure system, Barnstead/Thermolyne, Dubuque, Iowa, USA).

Isotherms were obtained on a computerized Nima Langmuir-Blodgett rectangular trough of 700 $cm^2$ (Model 601 BAM, Nima Technology LTD, Coventry, England) using a Wilhelmy plate to measure the surface pressure. In order to reduce contamination from dust, the trough was covered with a Plexiglas framework during isotherm measurements. It was also placed on an optical table to avoid mechanical vibrations. The temperature of the trough was kept constant with the aid of a water circulator bath. We measured the temperature of the subphase with an Omega thermometer (J-K-T Thermocouple, Stanford, CT, USA) covered with a Teflon tube, during each isotherm measurement. The subphase temperature was found to be constant within a precision of 0.1 K. Several isotherms of the films were obtained at four different temperatures, 10, 20, 30 and 40 °C, and were highly reproducible.

The water surface was aspirated with a Pasteur pipette before the deposition of each sample. The surface pressure was monitored while closing the barriers from the most expanded to the most compressed position. The samples were deposited on the water subphase only when the pressure readings were less than 0.2 mN/m at full compresion, and BAM images did not show any contamination on the water surface. 120 $\mu$l of cholesterol solution, at a concentration of 0.7764 mg $ml^{-1}$, were deposited gently drop by drop around the surface area of the subphase, using a 50 $\mu$l Hamilton microsyringe. We waited at least 20 min. to allow for the evaporation of the spreading solvent (chloroform) before compressing the monolayer. The isotherms were obtained by compressing the monolayer very slowly and continuously at a rate of 3-5 $Å^2$(molecule min.)$^{-1}$. We did not observe any dependence of the isotherms on compression rate.

During monolayer compression, the interface was analyzed by Brewster Angle Microscopy and null ellipsometer (BAM-ellipsometer, I-Elli2000, Nanofilm Technology GmbH, Germany) and real-time videos were recorded. For null ellipsometric measurements, we used an angle of the laser beam on the surface of 58°. We recall that the ellipsometric angles $\Delta$ and $\Psi$ are related to the ratio of the Fresnel reflection coefficients of the parallel ($R_p$) and normal ($R_s$) components, with respect to the plane of incidence, of the electric vector $\overrightarrow{E}$:

$$\tan\Psi\, e^{i\Delta} = \frac{R_p}{R_s}$$

Here $\tan\Psi$ is the measure of the change in the amplitude ratio before and after reflection and $\Delta$ is the change in phase difference between the two components caused by the reflection. The two ellipsometric angles, determined experimentally, are correlated to the refractive index and the thickness of the film. We analyzed the data with software based on a Fresnel algorithm developed by Nanofilm Technology GmbH as a part of the Ellipsometry module of the I-Elli2000. For cholesterol, we use a refractive index value of 1.47 [40].

The collapsed Langmuir films of cholesterol at the air/water interface were transferred onto a solid substrate (mica) in the upstroke mode, in this way obtaining the Langmuir-Blodgett films. The rate of transfer was set to 1 mm/min and freshly cleaved mica was used in every experiment. The transferred films were then taken to the atomic force microscope (AFM, Nanoscope IIIa, Digital Instruments, USA) for observation. We used both tapping and contact modes, and standard silicon nitride tips with a nominal spring constant of 40 and 0.12 $Nm^{-1}$, respectively. Measurements were performed with a 100-$\mu$m scanner. With the exception of flattening, AFM images have not been enhanced.

## 3. Results and Discussion

The pressure-area isotherms for cholesterol on a water subphase at 10, 20, 30 and 40°C are shown in Fig. 1, where the isotherms are practically identical. Therefore, the last three isotherms have been shifted to the right by 5 $Å^2$ $molecule^{-1}$ consecutively for clarity. In all cases, isotherms start at a very low surface pressure, near zero $mNm^{-1}$. These low surface pressures are typical when the gas phase (G) is present, which is corroborated by BAM observations; BAM images corresponding to points a-d in Fig. 1 from isotherm at 30°C are shown in Fig. 2. At low surface pressure we observed coexistence between the G phase and a liquid condensed phase (LC), as shown in Fig. 2a. Here, the dark areas are regions of low density and the white regions are large domains of the LC phase. The coexistence region ends at about 39.5 $Å^2$ $Molecule^{-1}$, where the isotherm shows a sharp

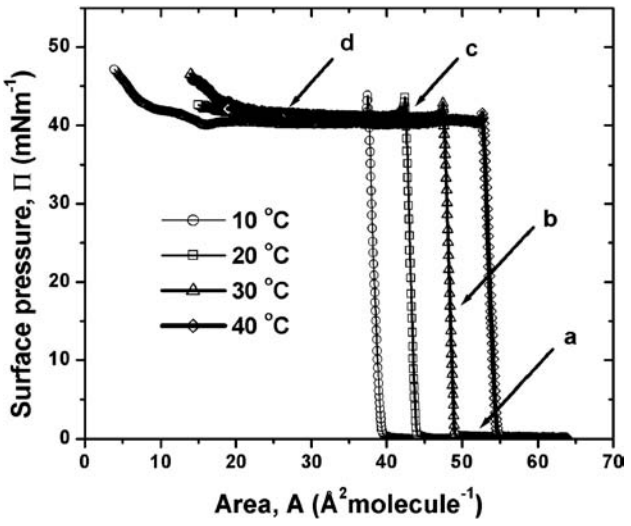


FIGURE 1. Surface pressure vs. area isotherms for Langmuir monolayers of cholesterol on a water subphase at 10, 20, 30 and 40°C, from left to right, respectively. Isotherms are quite similar in molecular area, therefore the last three isotherms have been shifted to the right by 5 $Å^2$$molecule^{-1}$ consecutively for clarity. The arrows show the position where images from Fig. 2 were taken.

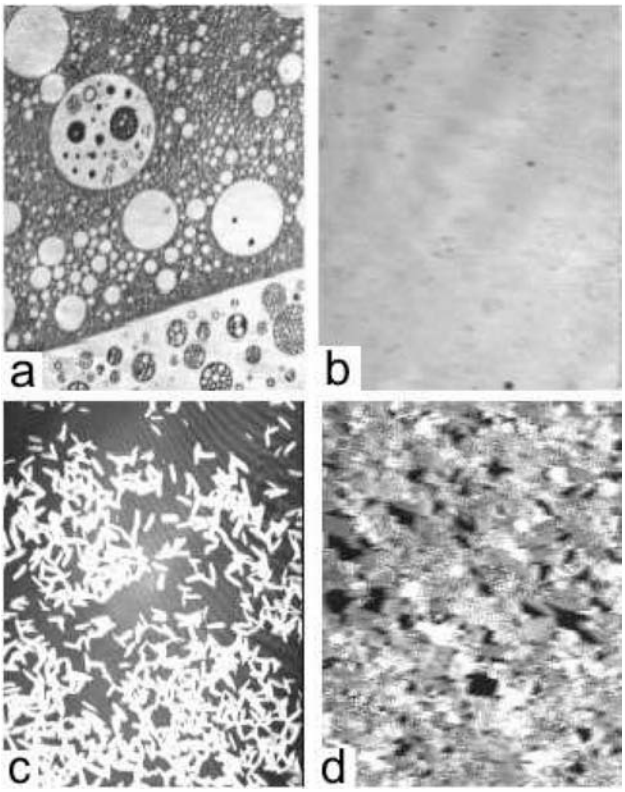


FIGURE 2. BAM Images of cholesterol films obtained along the isotherm of Fig. 1. They are 461.4 $\mu$m x 564.2 $\mu$m in size and they were taken with a 10x objective. 2a) Shows the coexistence of liquid condensed (LC) and gas (G) phases at surface pressure near 0 mN/m. The brightest circular domains and structures are the liquid condensed phase and the dark areas correspond to the G phase. 2b) Shows a typical image of the homogeneous LC phase during the sharp rise in surface pressure of the isotherms. Image 2c) shows th coexistence of the two-dimensional monolayer, dark areas, and three-dimensional crystals during collapse denoted by the plateau region at about 42 mN/m. Finally, one can see that the field of view is fill by three-dimensional crystals in image 2d).

pressure increase, to enter into the pure LC phase region where the BAM image becomes quite homogeneous, without contrast (see Fig. 2b). The fact that all isotherms are identical indicates that in the whole range of temperature we observe a transition between the LC and G phases; however, a liquid expanded (LE) might exist only a higher temperatures.

We moved the BAM analyzer to look for any molecular tilt anisotropy in the LC phase but we found none. Therefore, cholesterol molecules in this phase are untilted. Untilted phases normally have low compressibility and this explains why the surface pressure for cholesterol rises sharply. This compressibility coefficient is inversely proportional to the isotherm slope; when the slope is high, the compressibility is small, as is the case for cholesterol isotherms. This observation is also in agreement with GIXD experiments reported in Fig. 1b of Refs. (40) and (41), where the maximum of the Bragg rod peak appears at zero $q_z$ value, indicating the formation of an untilted phase. On further compression, the collapse pressure is reached at about 42 mNm$^{-1}$ and with an area, A = 38 Å$^2$molecule$^{-1}$, where both area and collapse pressure independent of temperature. This result is also consistent with that reported in Fig. 2a of reference [42]. Then, a long phase coexistence-like plateau appears at almost constant pressure. This could be taken as an indication of a first order 2D-3D phase transition. Indeed, BAM images taken at the start of the plateau, point c in Fig. 1, show the formation of large cholesterol crystallites seen as white domains in Fig. 2c, in coexistence with dark monolayer regions. Towards the end of the plateau, at point d in Fig. 1, BAM images show the surface almost completely covered by the crystallites, but the different gray levels indicate that the crystallites have different heights, as shown in Fig. 2d. Only at 40°C can we see a slight deviation from the general behavior of the rest of the isotherms towards the end of the 2D-3D coexistence plateau, where this isotherm remains flat towards the end, while the rest have a small increase in surface pressure at about 12 Å$^2$molecule$^{-1}$. This may be due to the metastability of cholesterol phases in the collapsed state.

On the other hand, some authors [43] have suggested that these types of isotherms are analogous to the mechanical response of the class of polymers referred to as tough plastics, which includes a yield stress and a plastic flow region. The plastic flow region is considered to be in a steady-state regime, where the observed stress remains constant when a constant strain rate is applied. For the monolayer system, it has been suggested that the overshot peak at collapse gives the value of the yield stress and that the plateau reflects a region of plastic flow. However, it is not possible to assert that the molecular mechanisms underlying the observed collapsed behavior of the monolayer are equivalent to those thought to occur for tough plastic polymeric films during tensile deformations. Linear polymers are inherently anisotropic and can form entanglements, which is not the case of cholesterol.

AFM observations of the transferred Langmuir-Blodgett films of cholesterol on mica reveal the microscopic shape and details of the crystals that were previously at the air/water interface. High molecular resolution AFM images were not possible to obtain, since the crystallites were too soft and were torn off by the AFM tip. Figs. 3a, c, e, and g, show the shape of the crystals formed during monolayer collapse, transferred at 35 Å$^2$ molecule$^{-1}$, at 10, 20, 30, and 40°C, respectively, which are large and have a plate-like shape. Initially, at the two lower temperatures, the crystals are homogeneous in height and made of two-layers only on top of the precursor monolayer, as shown in the analysis profile of these samples. This result is in agreement with those of Refs. 40 and 41 obtained at 5°C that reported the formation of a bilayer during cholesterol Langmuir monolayer collapse. However, at the two higher temperatures the crystallites are much larger, having several layers and sharp edges, as is also shown in the analysis profile of the corresponding images.

The initial plate-like crystals resemble the cholesterol monohydrate crystal. This is confirmed by measuring the angles of these crystals from several images, which turn out to be $100.3° \pm 2.1°$ and $81.5° \pm 0.9°$, which correspond to

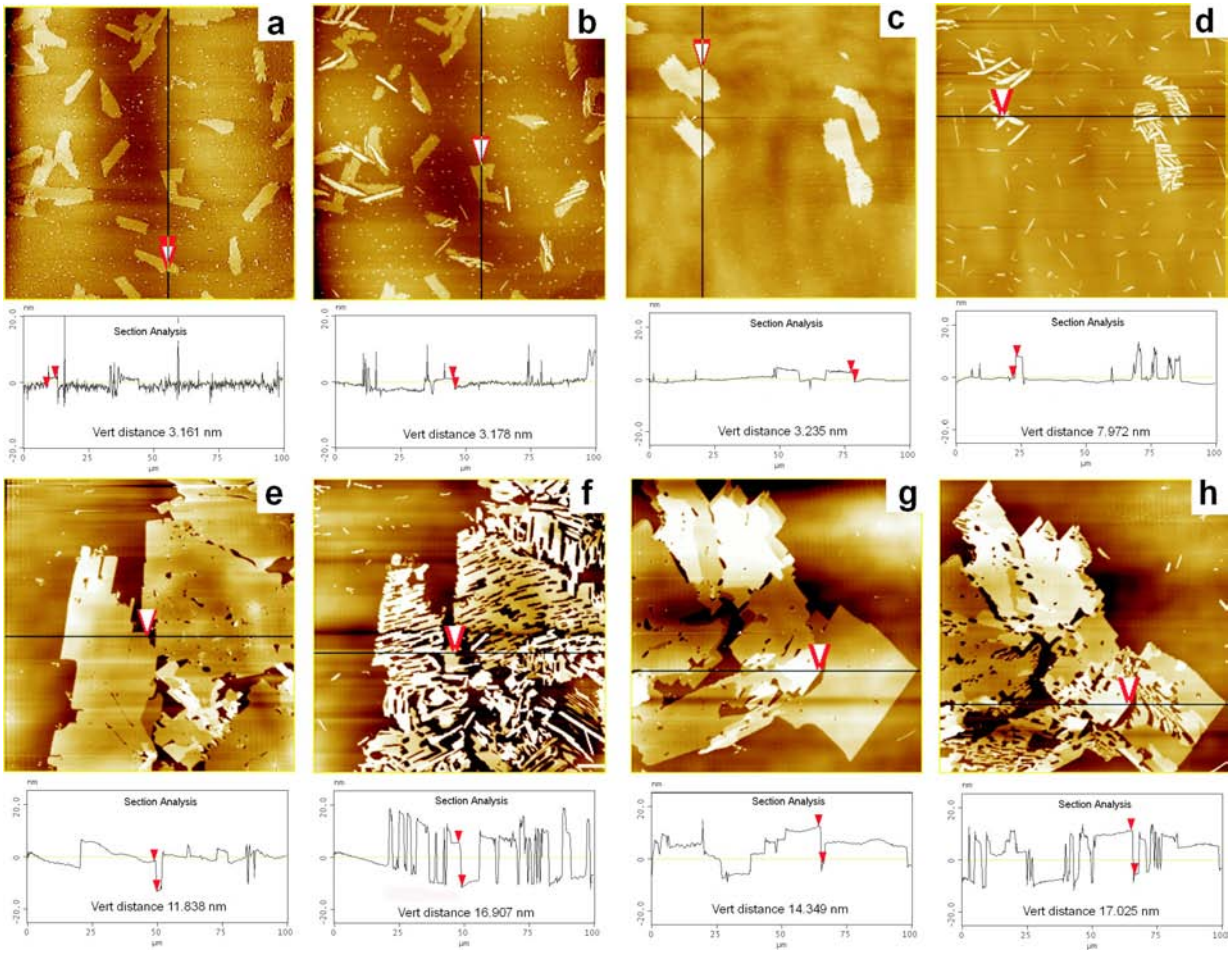


FIGURE 3. AFM images of the LB films transferred that show crystals that form after the collapse of the cholesterol monolayer (left column) and after the shape change of the collapsed crystals into bars (right). This phenomenon takes place at all temperatures as can be seen in this figure. a) and b) Correspond to crystals obtained at 10 °C, c) and d) 20°C, e) and f) 30°C and g) and h) 40°C. Images are $100\times100$ $\mu$m$^2$.

those of cholesterol monohydrate crystals [39]. However, during AFM scanning of the samples we observed a remarkable shape transition of the initial monohydrate crystals that are formed after collapse of the monolayer. Figs. 3b, d, f, and h show these shape changes of the crystal obtained at 10, 20, 30 and 40°C, respectively. As time passes, they transform into large, thin rectangular crystal bars. This transformation is spontaneous and independent of the scanning mode and the number of scannings; crystals from samples observed after several hours after transfer already showed a large change after the first scan.

This process takes place in all samples, as can be seen in this figure. However, some differences arise among the different temperatures. In general, at low temperatures (10 and 20°C), the initial crystals are smaller than at the higher temperatures and are formed only by a bilayer, which allows the final crystal bars to form easily, within a short time after transfer. On the other hand, at higher temperatures (30 and 40°C), the initial crystals are very large and made of several bilayers forming steps, these being steps large and homogeneous in height. These characteristics make the initial crystals at these temperatures more stable as function of time, avoiding their total fragmentation into crystal bars. It seems as if the fragmentation has begun, deep sharp clefts are formed, developing thin crystal bars between such clefts. The growing of both, clefts and bars, takes place along preferential orientations inside pre-existing crystallites, which likely reflect the internal preferential orientations of the crystalline structure. This shape change is halted at the steps that might represent a different orientation of the crystal, preventing the growing of the thinner crystal bars in that direction. In fact, the initiated bars between clefts are thicker than the original plate-like crystal in that region. It means that cholesterol molecules, that were initially where the clefts were formed, have gone up to the top of the incipient crystal bars. Therefore, possibly from this temperature upwards, the crystals are more stable, in the sense that they are not able to finish completely their transformation into isolated rectangular bars. In general, the bars are quite straight and thin. Moreover, some part of the monolayer crystallizes in the form of small but thick crystals bars with time, but not as a part of the collapse process, since they appear in areas where there was only a cholesterol monolayer, which dewets the mica surface to form the 3D crystal bars, as shown in Fig. 4.

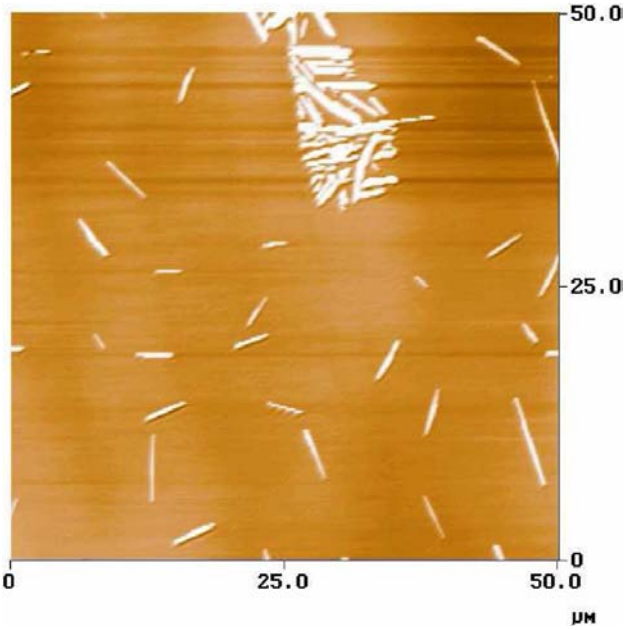


FIGURE 4. AFM image showing the rectangular shape of the needle-like anhydrous crystal bars formed from the metastable plate-like monohydrate crystals, similar to those crystals found in atherosclerotic plaques.

The question is now; what is the new phase that appears from the cholesterol monohydrate crystals? The transition from the monohydrate to the liquid-crystalline state of cholesterol occurs at 124°C and the transition between the low- and high-temperature anhydrous cholesterol crystal forms occurs at 39°C [39]. Since the AFM scanning is done at room temperature, it is most likely that the crystal bars are the low-temperature anhydrous crystalline form of cholesterol. Therefore, our results show that the initial plate-like crystals are metastable with respect to the needle-like crystal bars at these temperatures. Thus, monohydrate cholesterol is expected to be metastable, if present, at room temperature. Fig. 4 shows a close-up image of the needle-like crystal bars formed from the metastable plate-like crystals, where its rectangular shape, similar to those crystals found in atherosclerotic plaques, it can be observed.

We can establish two different mechanisms by which the crystal bars are formed. One is due to loss of water of the initial cholesterol monohydrate plate-like crystals obtained from the collapse of the Langmuir monolayer: as time passes, the plate-like crystals loss water and transform into crystal bars. The second one is a direct transformation of the 2-D monolayer into the thermodynamically stable crystal bars by a dewetting process of the mica surface. This indicates that even the transferred monolayer remains metastable against the formation of 3-D crystal bars. Our observations point out the important role that humidity plays in the stability of the cholesterol monohydrate. That is, it will spontaneously transform into anhydrous cholesterol crystal bars in environmental conditions when the humidity is low. Therefore, great care must be taken when handling cholesterol crystals, *e.g.* from human tissues, because changes can occur and therefore one can obtain erroneous conclusions if the humidity conditions during examination are not similar to those in the *in-vivo* tissues.

Figure 5 shows the thickness in nm of the crystals against the number of layers present in such crystals. Each data point represents the average of at least 20 measurements on different crystals of 3 AFM images. The thickness of a large crystal was measured in different positions, as well on different steps that showed different thicknesses. We see that the relation between these magnitudes is linear. In Fig. 5a, one such linear relation is presented for the initial cholesterol monohydrate crystals, before their morphological transformation into anhydrous needle-like crystals. The relation for the latter is shown in Fig. 5b. In the case of the monohydrate crystals, we found that all crystals at 10 and 20°C have the same height, around 3 nm. Therefore we do not show any relationship for them in Fig. 5a. In fact, at 10°C, their mean height is 3.16 $\pm$ 0.20 nm and at 20°C the mean height is 3.23 $\pm$0.62 nm. These two different behaviors in the thickness of the crystalline hydrates can be easily observed in the AFM images shown in Fig. 3 (a, c, e, and g). However, this behavior is puzzling and more experiments are needed to understand why the crystals show different thicknesses as a function of temperature. From the slope of the linear fits of those data shown in Fig. 5, we can deduce the thickness of a single layer of cholesterol.

So, at low temperatures, the monohydrate crystals are essentially formed by a bilayer of cholesterol on top of the precursor monolayer, where the top exocyclic octyl moieties are directed outwards to the hydrophobic air, whereas the hydroxyl moieties are sandwiched and thus protected from the hydrophobic air. This bilayer arrangement should be energetically more stable than one exposing the polar hydroxyl moieties to the hydrophobic air, as is proposed in Ref. 41. The thicknesses measured for each layer were 1.56$\pm$0.1 nm at 10°C and 1.61$\pm$0.31 nm at 20°C. However, at high temperatures, we show that the number of layers in monohydrate crystals is between 2 and 30, giving thicknesses of 1.64$\pm$0.03 nm and 1.66$\pm$0.01 nm, respectively. These values are close to the thickness of 1.695 nm obtained for bulk phases of monohydrate cholesterol obtained from X-ray measurements [44].

We performed a direct measurement of the crystallite thickness formed during collapse at the air/water interface by an independent ellipsometry method. At 20°C we obtained thickness values along the collapse plateau between 3.22 to 3.66 nm. At 30 and 40 °C we obtained discrete, much thicker values for the crystals. For example at 30°C we obtained thickness values like 18.85, 26.30, and 30.18 nm, while at 40°C we obtained 3.29, 6.67, 9.34, 12.66, and 15.28 nm. This mean that, along the plateau, the collapse process forms a bilayer on top of the monolayer at 20°C and lower temperatures, in good agreement with AFM measurements and with Refs. 40 and 41. However, the thickness of the collapse crystals increases significantly above 20°C. The difference in thickness obtained by ellipsometry at 30 and 40°C are due to

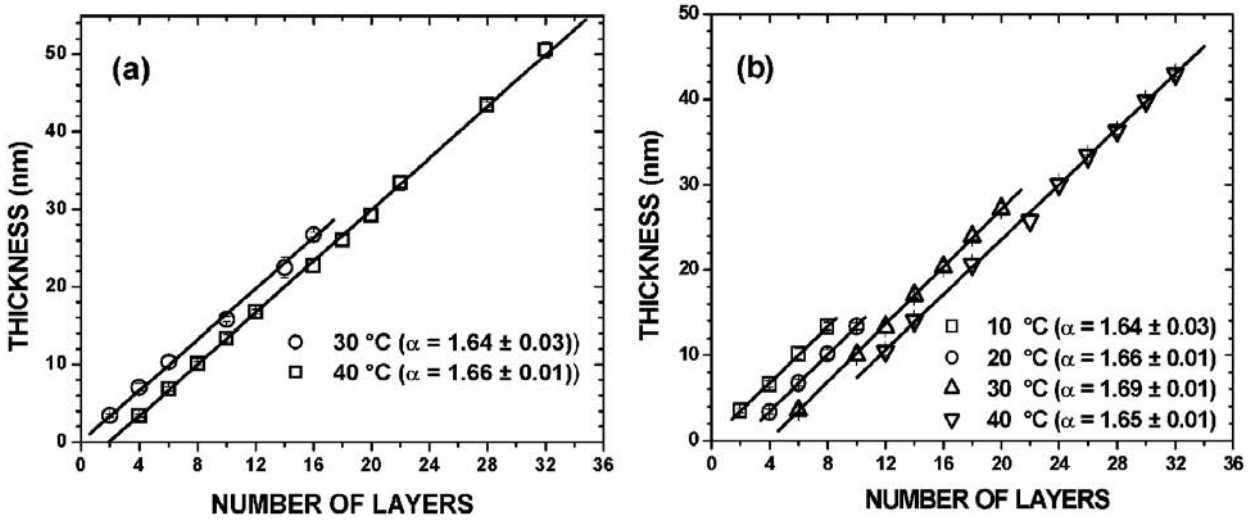


FIGURE 5. Linear relationship between the thickness of the crystal and steps against the number of layers ($\alpha$ is the slope of each line and represents the single cholesterol layer thickness). a). Initial plate-like crystallites of hydrated cholesterol, before their morphological transformation into needle-like crystals. We do not show the relation at 10 and 20°C since for those temperatures all crystals have the same thickness, around 3 nm, corresponding to two layers. b). Anhydrous cholesterol crystallites. The values for each sample were shifted by two layers from left to right for clarity.

the fact to measurements were taken towards the end of the plateau at 30°C, while at 40°C they were taken at the middle of the plateau.

If we now focus on the anhydrous-like crystallites (see Fig. 5b), we can observe that the number of layers present in the needle-shaped bars ranges from 2 to 26, which is much thicker than those crystals of the plate-like monohydrate crystalline. However, at the two lower temperatures the crystals tend to be thinner. The thickness for a single cholesterol layer in this phase ranges from 1.64±0.03 nm, 1.66±0.01 nm, 1.69±0.01 nm and 1.65±0.01 nm from the shape transformation of crystals transferred at 10, 20, 30 and 40°C, respectively. Again, these values are slightly lower than the thickness of 1.71 nm obtained for bulk phases of anhydrous cholesterol obtained from X-ray measurements [45,46].

The differences might be due in the difficulty of getting a lot of statistics on the different thicknesses of the crystals, and also tip effects might, on sharp crystals, increase the uncertainty in the measurements. However, an alternative interpretation of the fact that the actual thickness of the cholesterol layers in the crystals is less than the length of one cholesterol molecules is the possibility of interdigitation between the exocyclic octyl moieties in contact at the middle of each bilayer; but GIXD measurements [40] do not support this possibility.

The tendency of cholesterol to form multilayers with an even number of layers on top of the precursor monolayer, that is, with an integral number of bilayers, which are far more crystalline than the monolayer, highlights the fact that the hydroxyl moieties of the precursor monolayer must be directed toward the hydrophilic substrate, and the exocyclic octyl moieties of the outer layer must be toward the air.

From the rate at which the needle-shaped crystallites form during AFM scanning, we conclude that there seems to be a correlation between the rate of formation of crystal bars and the size of the initial plate-like monohydrate crystals. Those greater in size show a needle-crystal formation rate slower than smaller ones. This behavior may be due to the fact that the larger crystals are more stable than the smaller ones, preventing their large sizes from the tendency to build up of several cholesterol bilayers. In addition, the large crystals might have domain boundaries in different directions that could prevent the growth of large crystal bars in one direction, halting the total transformation of the plate-like crystal into isolated crystal bars, as happens at 30 and 40°C.

## 4. Conclusions

At the four temperatures studied, cholesterol isotherms first show a coexistence between a liquid condensed phase and gas phase, at a surface pressure near 0 mN/m. The analysis with BAM shows bright circular domains and larger structures corresponding to a liquid condensed phase coexisting with dark domains of the gas phase. Then, the coexistence ends at about 39.5 Å$^2$/Molecule when the isotherm enters the pure LC phase, which is a phase of low compressibility. The LC phase does not show molecular tilt-anisotropies in agreement with GIXD experiments [40, 41]. Finally, collapse occurs at about 42 mN/m showing a long plateau, analogous to a first order phase transition, where one coexistence phase is the 2D monolayer and the other one consists of 3D crystals. At the end of the plateau, the system is covered with three-dimensional crystallites of different heights, resembling a pure three-dimensional phase.

Therefore, this plateau in the cholesterol isotherms could be thought as of being similar to a 2D-3D first order phase transition. However, no dependence on temperature was found in the coexistence region as is typically the case, for example, in fatty acid Langmuir monolayers or more generally in bulk systems.

AFM observation of Langmuir-Blodgett films of cholesterol reveals initially the formation of large plate-like crystals, but long, break into large and thin crystal bars. This phenomenon takes place at all temperatures. We showed that the plate-like crystal formed during monolayer collapse correspond to the monohydrated cholesterol crystal form, while the crystals bars formed correspond to the low-temperature anhydrous cholesterol crystal form. Thus we present for the first time a direct observation of the phase change between these two cholesterol crystal forms. Moreover, we also observed that some crystals nucleate even from the monolayer, in the form of small needle-like crystals but with a very large height. The monohydrated cholesterol crystals transform into anhydrous cholesterol crystals by losing water molecules, while the monolayers do so by dewetting the mica surface.

Unexpectedly, all monohydrated crystals formed during collapse at 10 and 20°C have a height of around 3 nm, corresponding to a bilayer only. These results are in agreement with those reported by GIXD and reflectivity experiments obtained at 5°C [40, 41]. However, at the two higher temperatures, the crystals showed different heights; but there exists a linear relation between the thickness of the crystals and the number of layers present in such crystals from which one can estimate the thickness of a single crystal layer. This relation holds for the initial plate-like crystallites of the hydrate type and for their morphological transformation into needle-like crystals. The rate of morphological change from hydrated-like crystals into anhydrous-like crystals seems to depend on the size and height of the former: large, thick crystals transform more slowly while shallower and smaller crystal transform more quickly. We are investigating in detail the dynamics of this process. However, from this observation we can conclude that the plate-hydrate-like cholesterol crystals are metastable with respect to the thinner but thicker cholesterol needle-like crystals.

As we stated previously, anhydrous crystal bars similar to those found in this work appear in atherosclerotic plaques. In such plaques, the bars are apparently needle-shaped, but at higher magnification, they actually have a rectangular cross-section. Cholesterol crystals are also present in rheumatoid arthritis, but these crystals have a different shape from those found in atherosclerotic plaques. They are characterized by a broad square or rectangular plate-shape, similar to that found in this work immediately after collapse of the cholesterol monolayer. Thermodynamically, it is not obvious why both types of cholesterol crystals can be found in physiological samples. However, the local environment where these cholesterol crystal are found might help in the stabilization of both types of cholesterol crystals. In pure cholesterol samples, both types of crystal forms cannot exist at physiological temperatures, but some metastability can still be present that would explain their presence at these conditions as is shown by our results. In summary, we have presented studies of ultrathin cholesterol films, which show cholesterol crystals that are similar to those found in health issues; thus this kind of study is appealing in trying to understand cholesterol crystallization in physiological conditions.

## Acknowledgments

This work was financed by CONACYT (Grants NC72 and 45944), IMP Molecular Engineering Program and FAI-UASLP. J.M.M.-M. acknowledges support from the "Programa de Incorporación de Doctores Españoles a Universidades Mexicanas de AECI y ANUIES".

∗ e-mail: jaime@dec1.ifisica.uaslp.mx

1. S. Ryley, A.T. Chyla, and I.R. Peterson, *Thin Solid Films* **370** (2000) 294.
2. I.R. Peterson, *Molecular Electronics* (Research Studies Press: Taunton, U.K., 1992).
3. R. Bilewicz, T. Sawaguchi, R.V. Chamberlain, and M.Majda, *Langmuir* **11** (1995) 2256.
4. C.A. Nicolae, S. Cantin-Riviere, A. El Abed, and P. Peretti, *Langmuir* **13** (1997) 5507.
5. V. von Tscharner and H.M. McConnell, *Biophys. J* **36** (1981) 409.
6. M. Losche, E. Sackmann, and H. Möhwall, *Ber. Bunsenges. Phys. Chem.* **87** (1983) 848.
7. V.T. Moy, D.J. Keller, H.E. Gaub, and H.M. McConnell, *J. Phys. Chem* **90** (1986) 3198.
8. X. Qiu, J. Ruiz-García, K.J. Stine, J.V. Selinger, and C.M. Knobler, *Phys. Rev. Lett.* **67** (1991) 703.
9. S. Hénon and J. Meunier, *Rev. Sci. Instrum.* **62** (1991) 936.
10. D. Hönig and D. Möbius, *J. Phys. Chem.* **95** (1991) 4590.
11. D.K. Schwartz, J. Garnaes, R. Viswanathan, S. Chiruvolu, and J.A.N. Zasadzinski, *Phys. Rev. E* **47** 452.
12. K. Kjaer, J. Als-Nielsen, C.A. Helm, L.A. Laxhuber, and H. Möhwald, *Phys. Rev. Lett.* **58** (1987) 2224.
13. P. Dutta *et al.*, *Phys. Rev. Lett.* **58** (1987) 2228.
14. S. Ställberg-Stenhagen and E. Stenhagen, *Nature* **156** (1945) 239.
15. A.M. Bibo, C.M. Knobler, and I.R. Peterson, *J. Phys. Chem.* **95** (1991) 5591.
16. V.M. Kaganer, H. Möhwald, and P. Dutta, *Rev. Mod. Phys.* **71** (1999) 779.

17. M. Lundquist, *Chem. Scripta* **1** (1971) 5; *ibid* **1** (1971) 197.
18. R.D. Smith and J.C. Berg, *J. Colloid Interface Sci.* **74** (1980) 273.
19. D. Vollhardt, U. Retter, S. Siegel, *Thin Solid Films* **199** (1991) 189; D. Vollhardt and U. Retter, *Langmuir* **8** (1992) 309; S. Siegel, D. Hönig, D. Vollhardt, and D.Möbius, *J. Phys. Chem.* **96** (1992) 8157; D. Vollhardt, T. Kato, and M. Kawano, *Phys. Chem.* **100** (1996) 4141; D. Vollhardt, U. Retter, *Langmuir* **14** (1998) 7250.
20. T.R. Jensen, K. Kjaer, G. Brezesinski, J. Ruiz-García, H. Möhwald, N.N. Makarova, Godovsky, and K. Yu, *Macromolecules* **36** (2003) 7236.
21. E.S. Nikomarov, *Langmuir* **6** (1990) 410.
22. S.T. Milner, J.F. Joanny, and P. Pincus, *Europhys. Lett.* **9** (1989) 945.
23. D. Brown and E.J. London, *J. Membr. Biol.* **164** (1998) 103.
24. K. Simons and E. Ikonen, *Science* **290** (2000) 1721.
25. D.M. Small and G.G. Shipley, *Science* **185** (1974) 222.
26. D.M. Small, *Arteriosclerosis* **8** (1998) 103.
27. W. Guo, J. Morrisett, M. DeBakey, G. Lawrie, and J. Hamilton, *Artheroscler. Thromb. Vasc. Biol.* **20** (2000) 1630.
28. H. Bogren and K. Larsson, *Biochim. Biophys. Acta* **75** (1963) 65.
29. R.M. Epand, D. Bach, R.F. Epand, N. Borochov, and E. Wachtel, *Biophys. J.* **81** (2001) 1511.
30. T. Gilat and G.J. Sömjen, *Biochim. Biophys. Acta* **1286** (1996) 95.
31. G.J.Sömjen, Y. Ringel, F.M. Konikoff, R. Rosenberg, and T. Gilat, *J. Lipid Res.* **38** (1997) 1048.
32. F.M. Konikoff, H. Laufer, G. Messer, and T. Gilat, *J. Hepatol.* **26** (1997) 703.
33. P.R.C. Harvey, G.J. Sömjen, T. Gilat, S. Gallinger, and S.M. Strasberg, *Biochim. Biophys. Acta* **958** (1988) 10.
34. D.Q.H Wang and M.C. Carey, *J. Lipid Res.* **37** (1996) 2539.
35. F.M. Konikoff, D. Danino, D. Weihs, M. Rubin, and Y. Talmon, *Hepatology* **31** (2000) 261.
36. A. Kaplun *et al.*, *FEBS Lett.* **340** (1994) 78.
37. G.J. Sömjen *et al.*, *Biophys. J.* **68** (1995) 2342.
38. F.M. Konikoff, D.S. Chung, J.M. Donovan, D.M. Small, and M.C. Carey, *J. Clin. Invest.* **90** (1992) 1155.
39. C.R. Loomis, G.G. Shipley, and D.M. Small, *J. Lipid Res.* **20** (1979) 525.
40. S. Lafont *et al.*, *J. Phys. Chem B.* **102** (1998) 761.
41. H. Rapaport *et al.*, *Biophysical J.* **81** (2001) 2729.
42. E. Sparr, L. Eriksson, J.A. Bouwstra, and K. Ekelund, *Langmuir* **17** (2001) 164.
43. J.P. Kampf, C.W. Frank, E.E. Malmström, and C.J. Hamker, *Science* **283** (1999) 1730.
44. B.M. Craven, *Nature* **260** (1976) 727.
45. H.S. Shieh, L.G. Hoard, and C.E. Nordman, *Nature* **267** (1977) 287.
46. L.Y. Hsu and C.E. Nordman, *Science* **220** (1983) 604.